Investigation of recent weak single-pion production data

Jan T. Sobczyk and Jakub Żmuda
Institute of Theoretical Physics, University of Wrocław, pl. M. Borna 9, 50-204 Wrocław, Poland
(Received 30 January 2015; published 6 April 2015)

MiniBooNE [A. A. Aguilar-Arevalo *et al.* (MiniBooNE Collaboration), Phys. Rev. D **83**, 052007 (2011)] and MINERvA (B. Eberly *et al.*, arXiv:1406.6415v2 [hep-ex]) charge current π^+ production data in the Δ region are discussed. It is argued that despite the differences in neutrino flux, they measure the same dynamical mechanism of pion production and should be strongly correlated. The correlation is clearly seen in the Monte Carlo simulations done with the NuWro generator but is missing in the data. Both the normalization and the shape of the ratio of measured differential cross sections in pion kinetic energy are different from the Monte Carlo results; in the case of normalization the discrepancy is by a factor of 1.49.

DOI: 10.1103/PhysRevC.91.045501 PACS number(s): 13.15.+g, 13.60.Le, 24.10.Lx, 25.30.Pt

I. INTRODUCTION

A lot of effort has been made to better understand single-pion production (SPP) reactions in neutrino-nucleon and -nucleus scattering. These studies are motivated by the demand to reduce systematic errors in neutrino oscillation experiments. In the few-GeV energy region characteristic of experiments such as T2K [1], NOvA [2], LBNE [3], and MicroBooNE [4], the SPP channels account for a large fraction of the cross section (at 1 GeV on an isoscalar target, about 1/3 of the cross section).

In the 1-GeV energy region the dominant SPP mechanism is through Δ excitation. There are several challenges in the theoretical description of the SPP reaction in the Δ region. One comes from uncertainties in the N-Δ transition matrix element, mainly due to the lack of precise information on its axial part. In order to describe the SPP channels one also needs a significant nonresonant background contribution. Several theoretical models have been developed (see Refs. [5]) to predict its shape and magnitude. The differences among them introduce an important model dependence in the N-Δ transition matrix element analysis and even in the description of the Δ resonance.

In theoretical computations of SPP on atomic nuclei nuclear effects must be incorporated starting from the Fermi motion and Pauli blocking. It is very important to include the in-medium Δ self-energy. Its real part shifts the pole, whereas the imaginary part corresponds to medium-modified SPP and pionless Δ decay processes. The problem of charge current SPP on nuclei is addressed in Refs. [6] by assuming Δ dominance with many-body effects taken from Ref. [7]. The computations suggest a significant reduction in the pion production cross section.

On top of all that, in the impulse approximation regime final-state interaction (FSI) effects must be carefully evaluated (see, e.g., Ref. [8]). FSIs include pion rescattering, absorption, charge exchange, and (for sufficiently high energies) production of additional pions. The nuclear physics uncertainties are so large that in most cases experimental groups do not try to measure the characteristics of the neutrino-nucleon SPP process. They publish instead the cross-section results with all the nuclear effects included with signal events defined by outgoing pions.

More precise SPP measurements on both nucleon and nucleus targets are necessary. Models of Δ excitation matrix elements and nonresonant background are still validated mainly based on the old low-statistics bubble chamber experiments performed at Argonne National Laboratory (ANL [9]) and Brookhaven National Laboratory (BNL [10]). The nonresonant background is more important in neutrino-neutron SPP channels, where the cross sections are smaller, than in neutrino-proton SPP reactions, and the statistical uncertainties are larger [11,12].

In view of these limitations it is important to explore the information from more recent neutrino-nucleus cross-section measurements. In the case of a charged-current $1\pi^+$ production reaction on a carbon target interesting studies were done by the MiniBooNE [13] and MINERvA [14] collaborations. Both analyses focus on the Δ region. The main difference is in the neutrino energy. Typical MiniBooNE interacting neutrino energies are lower by a factor of ∼4–5.

The main results of this paper are as follows. According to Monte Carlo (MC) simulations a strong correlation between the differential cross sections in pion kinetic energy in the two experiments is expected. The MINERvA cross section is expected to be larger by a factor of ∼2. The shape of the differential cross sections is anticipated to be very similar. This correlation is absent in the published data. The data/MC discrepancy is seen in a particularly clear way when one compares the ratio of differential cross sections from the two experiments with the MC predictions. The experimental quantity is far from the anticipated value of ∼2. Also, the shapes of predicted and measured ratios are different.

The paper is organized as follows: In Sec. II MiniBooNE and MINERvA SPP data are discussed and rebinning of the MniBooNE data according to the MINERvA bins is done. A MC-data comparison is presented in Sec. III, with the main result reported in Sec. III A. In Sec. IV we conclude our paper.

II. MiniBooNE AND MINERvA SPP DATA

The MiniBooNE measurement was done on a mineral oil target (CH_2). The neutrino flux peaks at ∼700 MeV, with the tail extending to 3 GeV. The signal events are defined as $1\mu^-$, $1\pi^+$ and no other mesons in the final state.

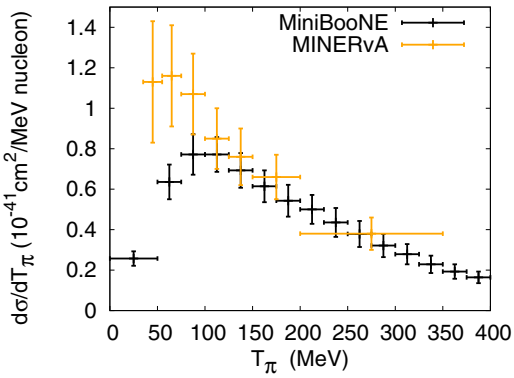

FIG. 1. (Color online) Differential cross section in pion kinetic energy. MiniBooNE data points are taken from Ref. [13]; MINERvA, from Ref. [14].

The MINERvA measurement was done on a CH target with a larger energy flux, peaking at ∼3 GeV and with a long high-energy tail. Signal charged-current events contain exactly one charged pion, almost always π^+. Due to the cutoff on invariant hadronic mass $W < 1.4$ GeV, contamination from the $1\pi^\pm 1\pi^0$ events is very small.

In both cases the signal includes a fraction of coherent π^+ production events.

Even though in the MiniBooNE measurement typical neutrino energies are lower by a factor of ∼4–5 compared to the MINERvA energies, in both experiments the dominant contribution comes from $\Delta(1232)$ excitation. In both cases the target consists mostly of carbon and we expect a lot of similarity in the measured cross sections. According to NuWro MC simulations the only significant difference in the two measurements comes from overall normalizations. Typical MiniBooNE ν_μ energies are closer to the pion production threshold energy. From the ANL and BNL experiments it is known that with a cutoff $W < 1.4$ GeV, π^+ production cross sections at ∼700 MeV and ∼4 GeV differ by a factor of ∼2.

The cross section results from the two experiments are shown in Fig. 1. Errors are given as a fractional uncertainty for each bin.

We would like to perform a direct comparison between experimental results and MC simulations. Later, we focus on the ratio of measured cross sections. However, the two experiments have different binning and the ratio cannot be computed without appropriate mapping of one result onto the other. In order to avoid any bias we decided to proceed as carefully as possible. MiniBooNE binning is finer than MINERvA, hence we "translate" the MiniBooNE data to the MINERvA bins.

In Fig. 1 we see that in most cases MINERvA bins overlap with at most two MiniBooNE bins. We use a linear interpolation of the cross section and its error. The measured points can be correlated, but there is no available information about the covariance matrix for considered data. This procedure is justified if the new bin contains data from two bins and cannot be applied to combine a higher number of bins.

In the latter case we use the following method. We assume that each data point represents a random variable with an expected value equal to the central value [cross section in the i-th bin, $E(X_i) = \sigma(E_i)$] and variance equal to the squared error [$\mathrm{Var}(X_i) = (\Delta\sigma_i)^2$]. The ith MiniBooNE bin contributes to the jth MINERvA bin with a weight equal to the ratio of the bin's intersection α_{ij} with the MINERvA bin to the MINERvA bin width W_j:

$$w_{i,j} = \frac{\alpha_{i,j}}{W_j}. \tag{1}$$

The expected value of the MiniBooNE cross section in the jth MINERvA bin is

$$E(Y_j) = E\left(\sum_i w_{ij} X_i\right) = \sum_i w_{ij} E(X_i). \tag{2}$$

In the above equation $E(X_i)$ represents the measured MiniBooNE cross section. The variance of the sum of N random variables is

$$\mathrm{Var}\left(\sum_{i=1}^{N} w_{i,k} X_i\right) = \sum_{i=1}^{N} w_{i,k}^2 \mathrm{Var}(X_i) + 2\sum_{i>j} w_{i,k} w_{j,k} \mathrm{Cov}(X_i, X_j). \tag{3}$$

Unfortunately, the MiniBooNE experiment did not publish the covariance matrix. The experimental errors are almost entirely systematic. The simplest assumption, $\mathrm{Cov}(X_i, X_j) = 0$, would reduce the error during the rebinning operation, since $w_{ij} \leqslant 1$. A reasonable assumption for these systematic errors is that if one combines the neighboring bins, the resulting error is a weighted average of the contributing bin errors. It is easy to show that if one sets $\mathrm{Cov}(X_i, X_j) = \sqrt{\mathrm{Var}(X_i)\mathrm{Var}(X_j)}$, the resulting error will be exactly a weighted average:

$$\begin{aligned}\mathrm{Var}\left(\sum_{i=1}^{N} w_{i,k} X_i\right) &= \sum_{i=1}^{N} w_{i,k}^2 \mathrm{Var}(X_i) + 2\sum_{i>j} w_{i,k} w_{j,k} \sqrt{\mathrm{Var}(X_i)\mathrm{Var}(X_j)} \\ &= \sum_{i=1}^{N} w_{i,k}^2 (\Delta\sigma_i)^2 + 2\sum_{i>j} w_{i,k} w_{j,k} \Delta\sigma_i \Delta\sigma_j \\ &= \left(\sum_{i=1}^{N} w_{i,k} \Delta\sigma_i\right)^2. \end{aligned} \tag{4}$$

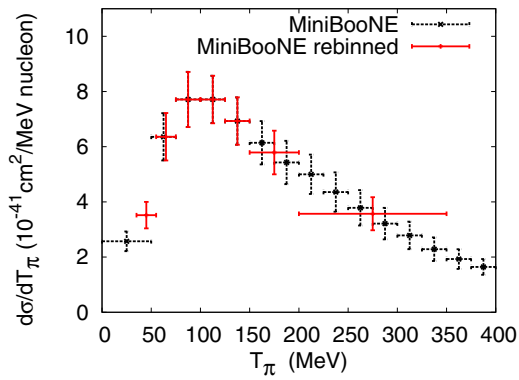

FIG. 2. (Color online) MiniBooNE differential cross section in pion kinetic energy taken from Ref. [13], rebinned into MINERvA-sized bins.

The new data binning for the MiniBooNE experiment according to Eqs. (2) and (4) is shown in Fig. 2. After rebinning, the systematic errors are not reduced, as expected.

III. NuWro MONTE CARLO EVENT GENERATOR

NuWro is a versatile MC simulation tool describing lepton-nucleon and lepton-nucleus interactions in the energy range from ∼100 MeV to 1 TeV. Its main functionalities and implemented physical models are presented in Ref. [15]. Neutrino-nucleon interaction modes are quasielastic [QEL (or elastic for neutral current (NC)]; resonant (RES), covering $W < 1.6$ GeV; and DIS, defined as $W > 1.6$ GeV. For the purpose of this study the anisotropy in the pion angular distribution in Δ decay events has been implemented using the density matrix elements measured in ANL [9] and BNL [10] experiments.

For neutrino-nucleus scattering the impulse approximation is assumed. New reaction modes, absent in neutrino-nucleon scattering, are coherent pion production (COH) and two-body current interactions on correlated nucleon-nucleon pairs (MEC). In our simulation we used the Valencia MEC model [16] with the momentum transfer cutoff $|\vec{q}| < 1.2$ GeV, as suggested in Ref. [17]. In MEC events final-state nucleons are described using a model proposed in Ref. [18].

The primary interaction is followed by hadron rescatterings (FSIs) simulated by the custom-made internuclear cascade model [15].

In the simulations discussed in this paper the carbon nucleus is treated within the relativistic Fermi gas model. Δ in-medium self-energy effects are included in an approximate way using the results from Ref. [19]. The simulations are carried out for composite targets CH_2 (MiniBooNE; strictly speaking, the target is $CH_{2.08}$, but it is a negligible effect) and CH (MINERvA), thus they contain both free proton and carbon contributions. Each interaction mode is computed separately with 10^6 events.

According to NuWro simulations, in the MiniBooNE and MINERvA experiments pion production signal events originate from the following.

(i) RES interactions contribute, typically through Δ excitation and decay, but also with some contribution from the nonresonant background. According to NuWro, RES accounts for 87.1% and 84.7% of the signal for the MiniBooNE and MINERvA experiments, respectively. There is a very important impact of FSI effects on the final-state pion production rate because many pions are absorbed or suffer from the charge exchange reaction inside the carbon nucleus.

(ii) The COH process populates 6.7% (MiniBooNE) and 10.7% (MINERvA) of the signal. NuWro uses the Rein-Sehgal COH model from Ref. [20] with the lepton mass correction from Ref. [21]. Comparison with the recent MINERvA COH measurement published in Ref. [22] suggests that NuWro may overestimate the experimental data.

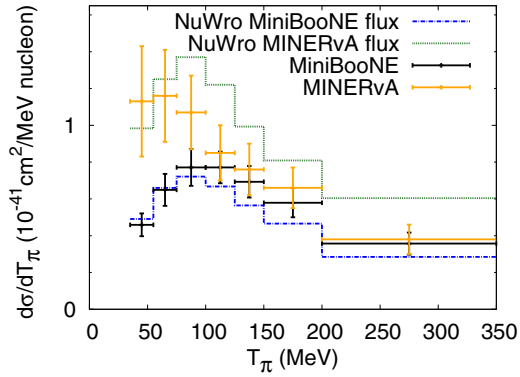

FIG. 3. (Color online) Differential cross section in pion kinetic energy. MiniBooNE and MINERvA data points are shown together with NuWro predictions.

(iii) DIS interactions contribute only to the MiniBooNE signal, at the level of 3.6%. A typical scenario is that one of two pions produced in the primary interaction is absorbed.

(iv) QEL and MEC interactions with pions produced due to nucleon rescattering reactions account for 2.7% of MiniBooNE and 4.6% of MINERvA signal events.

Results of the NuWro simulations together with the experimental points are shown in Fig. 3. The MC predictions tend to overestimate the MINERvA data and underestimate the MiniBooNE data at the same time. In the case of MiniBooNE results similar problems have been reported for many theoretical models (see e.g., Refs. [23] and [24]). Another observation is that the Monte Carlo simulation predicts a large difference between the MiniBooNE and the MINERvA cross sections over the whole pion kinetic energy range. On the other hand, in Fig. 3 one can see that for higher pion kinetic energies, values reported in both experiments are very similar. Also, in the MC simulations the differential cross sections tend to peak at the same point in pion kinetic energy, near the threshold for Δ production, which, in the pion FSI simulations, leads to significant pion absorption. However, both of the experimentally measured cross sections seem to reach their maximal values at different points. This is not very strongly pronounced in Fig. 3, because the MINERvA errors are very large. We checked that introduction of the anisotropy for the pion angular distribution does not change the NuWro results much, giving an effect of, at most, 10% in a few kinetic energy bins but typically much smaller. The shapes of differential cross sections change a little but there is almost no structure to it save for the kinetic energy distribution. We observe there a shift of the cross section by ∼5% towards higher kinetic energies in both MINERvA and MiniBooNE distributions.

The NuWro results look consistent with the GENIE [25] predictions for $\frac{d\sigma}{dT_\mu}$, shown in Fig. 4 of Ref. [14]. NuWro and GENIE use different physical models to describe SPP (GENIE relies on the resonant Rein-Sehgal model) but both

predict a strong correlation between results from the two experiments.

A. Ratio of MINERvA/MiniBooNE cross section in pion kinetic energy

Correlations of both π^+ production measurements should be clearly seen in the ratios of measured differential cross sections in pion kinetic energy relative to the neutrino flux from the two experiments. Their shapes do not depend on the overall normalizations in the two experiments.

In order to calculate the ratios of both measurements together with the appropriate errors we consequently treat the processed data points as random variables X and Y with known expected values and variances. One has to compute $E(\frac{X}{Y})$ and $\mathrm{Var}(\frac{X}{Y})$. For independent variables,

$$E(X \cdot Z) = E(X)E(Z), \tag{5}$$

$$\mathrm{Var}(X \cdot Z) = \mathrm{Var}(X)\mathrm{Var}(Z) + E(X)^2\mathrm{Var}(Z) + E(Z)^2\mathrm{Var}(X), \tag{6}$$

and the replacement $Z = \frac{1}{Y}$ must still be done.

The assumption that the two experiments are independent is rather conservative because errors coming from neutrino interaction models are correlated in both cases.

The most difficult task is to calculate $E(\frac{1}{Y})$ and $\mathrm{Var}(\frac{1}{Y})$, because $E(\frac{1}{Y}) \neq \frac{1}{E(Y)}$ unless the probability distribution function of Y is given by the Dirac δ function, $P(Y) = \delta(Y - Y_0)$. We must introduce some model dependence, which, fortunately, is shown to be negligible.

We investigated several assumptions for the $P(Y)$:

(i) flat distribution,
(ii) linear distribution,
(iii) quadratic distribution, and
(iv) log normal distribution.

The assumption is that $P(Y \leqslant 0) = 0$ and $P(Y)$ drops to 0 more rapidly than Y^2 as Y approaches 0 since the cross section cannot be negative and we do not want the integral to give indefinite values for $E(1/Y)$ and $E(1/Y^2)$.

We tested the model dependence of ratios using the above probability distribution hypotheses by calculating both the expected ratio value and its error. We compared them also to a "naive" approximation, in which $E(\frac{1}{Y}) \approx \frac{1}{E(Y)}$ and $\mathrm{Var}(\frac{1}{Y}) \approx \frac{1}{\mathrm{Var}(Y)}$.

We verified that the expectation values and variances coming from various probability distribution hypotheses do not differ in any significant manner. The only exception is the "naive" approach, leading to a few-percent effect on the expected value and an increase in the variance. Of the above-described models we chose the log-normal distribution, as it allows any value of random variable along the positive real semiaxis. It has the functional form, expected value, and variance

$$P(Y) = \frac{1}{\sqrt{2\pi}bY}\exp\left[-\frac{(\ln(Y)-a)^2}{2b^2}\right]\Theta(Y),$$
$$E(Y) = \exp(b^2/2 + a), \quad \mathrm{Var}(Y) = \exp(2b^2 + 2a). \tag{7}$$

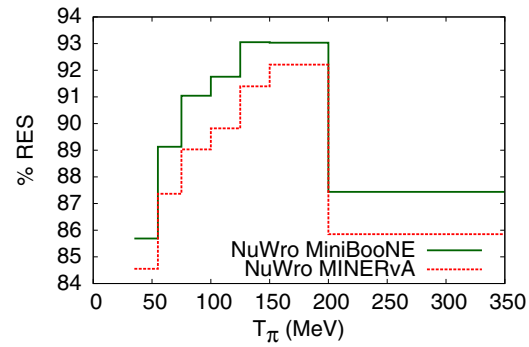

FIG. 4. (Color online) Contributions from the RES channel to MiniBooNE and MINERvA differential cross sections in pion kinetic energy as predicted by NuWro.

From the above equation we get $E(\frac{1}{Y}) = \exp(b^2/2 - a)$ and $\mathrm{Var}(\frac{1}{Y}) = \exp(b^2 - 2a)[\exp(b^2) - 1]$.

The procedure is to generate samples with the NuWro generator for both experiments and compare the resulting ratio of MC cross sections to the experimental ratio. In order to maintain statistically meaningful samples each dynamical channel contributing to the MINERvA and MiniBooNE signals was generated separately.

We tried to estimate the errors of both ratios as calculated by NuWro. We distinguish systematic and statistical errors coming from the implemented theoretical models. We run the simulations with a high event rate in order to minimize statistical fluctuations. We obtained at least 8000 events in each bin, with a typical value of the order of 10^4–10^5 events per bin. The resulting impact of statistical errors on the predicted ratio is negligible.

In order to establish the leading systematic errors we identified a dominant dynamical process giving rise to the signal in both experiments. The contributions from the RES channel usually exceed 85%–90% (see Fig. 4). We conclude that most of the MiniBooNE and MINERvA signal events originate from the same physical processes. The pion kinetic energy distribution produced in the RES process before FSI is quite similar for the two experiments (see Fig. 5). Thus we expect that the impact of pion FSI effects is also similar in both cases. Reference [14] reports that according to GENIE 24% of the MiniBooNE signal events correspond to $W > 1.4$ GeV. In NuWro simulations the fraction is 23%.

For the NuWro ratio results we used a simplified MC systematic error analysis based on uncertainties in the RES process, which should cover the leading error of MC predictions. Two error sources are taken into account:

(i) Δ production rate uncertainty, driven by C_5^A and $M_{A\Delta}$ parameters, and
(ii) Δ decay uncertainty, coming from pion angular correlations.

We varied the axial coupling of the Δ resonance $C_5^A(0) = 1.19 \pm 0.08$ and $M_{A\Delta} = 0.94 \pm 0.03$ (GeV) within the limits found in Ref. [26] and treated the maximum variation as systematic errors $\delta_{C_5^A}$ and $\delta_{M_{A\Delta}}$. We also compared the pion angular distribution anistotropy measured by ANL

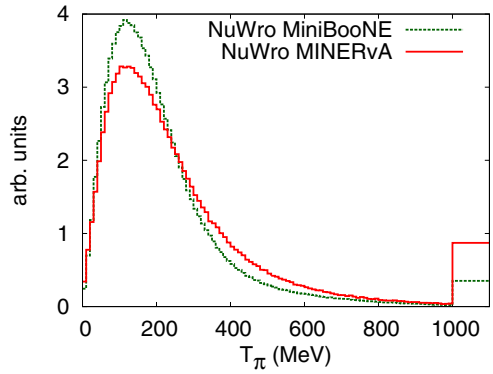

FIG. 5. (Color online) Spectrum of the pion kinetic energy for MiniBooNE and MINERvA as predicted by NuWro without FSI effects. The last bin combines pions with kinetic energies above 1 GeV.

and BNL experiments. Its maximum variation from both parametrizations has been taken as another systematic error, δ_{decay}. We combined these errors in quadrature and obtained the estimate of the total error in NuWro simulations $\delta_{\text{MC}} = \sqrt{\delta^2_{C_5^A} + \delta^2_{M_{A\Delta}} + \delta^2_{\text{decay}}}$.

In Fig. 6 we show the final results for

$$\frac{\left(\frac{d\sigma}{dT_\pi}\right)^{\text{MINERvA}}}{\left(\frac{d\sigma}{dT_\pi}\right)^{\text{MiniBooNE}}},$$

where the experimental results are compared to the NuWro predictions. NuWro central results are obtained with BNL angular correlations and default values of $C_5^A(0) = 1.19$ and $M_{A\Delta} = 0.94$ GeV.

It is essential to look independently for the shape of the ratio. Differences in shape are perhaps more important than discrepancies in overall scale, which can be due to uncertainties in overall cross-section normalizations in the two experiments. In the case of the MINERvA measurement the overall normalization error can be estimated as $\sim$15% (flux error, correction for muon angles exceeding 20°, detector effects) [27]. The MiniBooNE normalization error should be similar in size. In order to compare the shapes of two ratios

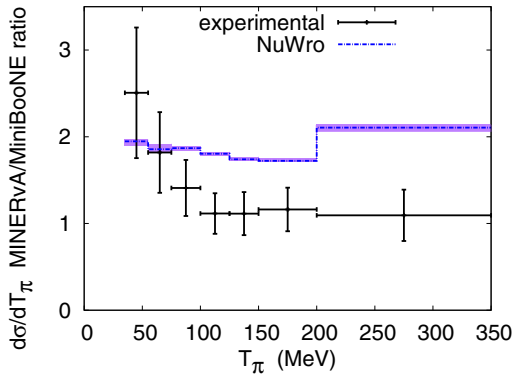

FIG. 6. (Color online) Ratios of differential cross sections in pion kinetic energy from MINERvA and MiniBooNE experiments together with NuWro predictions.

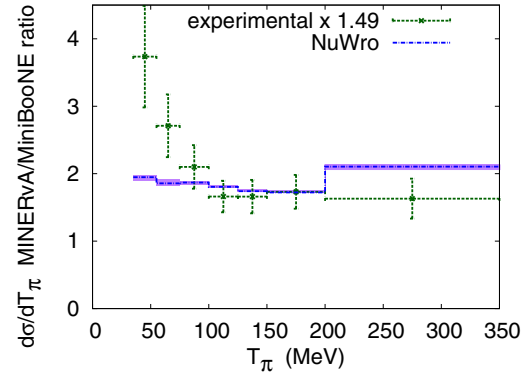

FIG. 7. (Color online) The same as Fig. 6, but with experimental results rescaled by a factor of $\eta = 1.49$.

we introduced a scaling factor η and found its value by trying to adjust the experimental results and NuWro predictions.

We obtained the best-fit value $\eta = 1.49 \pm 0.15$. The value of η is surprisingly large compared to the estimated normalization error from the two experiments. Also, the shapes of measured and NuWro-predicted ratios of cross sections in the function of pion kinetic energy are different; see Fig. 7, where rescaled experimental results together with NuWro predictions are shown.

In the past GENIE [25] and GiBUU [23] also had problems with understanding π^+ production data. In the case of GiBUU, in [23] the paradoxical conclusion was drawn that the MiniBooNE data are reproduced better if FSI effects are neglected. There are differences in the underlying SPP and FSI models in all the generators, and the model that is implemented in NuWro can be improved in many respects. Nevertheless, it seems unlikely that such a large data/MC discrepancy is caused only by deficiencies of the NuWro treatment of neutrino pion production. The main argument is that in the cross-section ratios all the implemented model defects should roughly cancel each other because in both cases the dominant dynamical mechanism, Δ excitation and decay, is exactly the same, and also the FSI effects are expected to be very similar.

B. Pion angular distribution

We studied also the pion angular distribution in both experiments. In the case of the MiniBooNE experiment the points for the pion angular distribution are taken from M. Wilking's Ph.D. thesis [28]. These data must be considered with caution, as even though they are public, they are not official MiniBooNE results.

The first problem is that the MiniBooNE detector has little sensitivity to the pion direction near the Cherenkov threshold at $T_\pi \sim 70$ MeV. This results in a cutoff at a pion kinetic energy of 150 MeV in the double-differential cross section presented in Table XVII of Ref. [13]. The second problem is that Ref. [28] does not include improvements coming from better algorithms to separate muons and charged pions, which have some impact on the unfolded pion differential cross section.

For the second problem we looked at the overlapping kinematical region from Ref. [28] and the MiniBooNE paper

[13] for pion double-differential cross-section results. The agreement is at the level of ∼1%–6%.

As for the first problem we used the NuWro MC generator to estimate the range of pion production angles, Θ_π, for which $T_\pi < 150$ MeV events do not dominate. We noticed a general pattern that more energetic pions preferably move in the forward hemisphere, and less energetic pions in the backward hemisphere. This can be understood as an effect of a boost of mostly uniform distribution of pions in the Δ resonance rest frame to the laboratory frame.

We observed that for pion production angles $\lesssim 70^\circ$ the fraction of near-threshold pions does not exceed 13% and the contribution of pions with kinetic energies below 150 MeV is less than ∼50%. It is plausible that the data from Ref. [28] are trustworthy for $\Theta_\pi \lesssim 70^\circ$ and we compared them with the MINERvA results. As before, we calculated ratios of experimental results to MC predictions. The conclusion is that there is a significant disagreement in shape. NuWro predicts that the ratio should be roughly equal to 2 for $\Theta_\pi \in [0^\circ, 70^\circ]$. On the contrary, the experimentally measured ratio $(\frac{d\sigma}{dT_\pi})^{\text{MINERvA}}/(\frac{d\sigma}{dT_\pi})^{\text{MiniBooNE}}$ shows a strong drop, from the value of ∼2.5 for $\Theta_\pi = 0^\circ$ to ∼0.8 for $\Theta_\pi \approx 50^\circ$.

IV. CONCLUSIONS

A comparison of experimental π^+ production data from MiniBooNE and MINERvA experiments reveals that there is a large (factor of 1.49) normalization discrepancy between the two measurements. There are also noticeable differences in the measured shapes of differential cross sections in pion kinetic energy. Unfortunately, the MiniBooNE Cherenkov detector does not provide us with a reliable angular distribution due to the near-threshold effects and we cannot make any definite conclusions regarding this observable.

We are still far away from a good understanding of SPP channels in neutrino scattering in the Δ region. Interpretation of the old ANL and BNL deuteron target experiments is not straightforward because of apparent differences in measured cross sections (see, however, the discussion in Refs. [26] and [29]) and problems with modeling nonresonant contributions [12]. It is clear that a more dedicated experimental effort aiming to measure pion production reactions together with nuclear effects is needed.

ACKNOWLEDGMENTS

We thank B. Eberly and S. Dytman for useful comments on the MINERvA experiments and M. Wilking for comments on the MiniBooNE experiments. We also thank Barbara Szczerbinska for warm hospitality at the CETUP*2014 (Center for Theoretical Underground Physics and Related Areas) workshop in South Dakota, where the idea of this study was conceived. Both authors were supported by NCN Grant No. UMO-2011/M/ST2/02578.

[1] K. Abe *et al.* (T2K Collaboration), Nucl. Instrum. Meth. A **659**, 106 (2011).
[2] D. Ayres *et al.*, arXiv:hep-ex/0503053v1.
[3] C. Adams *et al.*, arXiv:1307.7335v3 [hep-ex].
[4] H. Chen *et al.*, Nucl. Instrum. Meth. A **623**, 391 (2010).
[5] S. L. Adler, Ann. Phys. **50**, 189 (1968); G. L. Fogli and G. Nardulli, Nucl. Phys. B **160**, 116 (1979); D. Rein, Z. Phys. C **35**, 43 (1987); T. Sato, D. Uno, and T. S. H. Lee, Phys. Rev. C **67**, 065201 (2003); T. Sato and T.-S. Lee, Int. J. Mod. Phys. A **20**, 1668 (2005); E. Hernandez, J. Nieves, and M. Valverde, Phys. Rev. D **76**, 033005 (2007); A. Mariano, Nucl. Phys. A **790**, 267c (2007).
[6] S. K. Singh, M. J. Vicente-Vacas, and E. Oset, Phys. Lett. B **416**, 23 (1998); **423**, 428 (1998); S. Ahmad, M. S. Athar, and S. K. Singh, Phys. Rev. D **74**, 073008 (2006); M. Sajjad Athar, S. Chauhan, and S. K. Singh, J. Phys. G **37**, 015005 (2010).
[7] E. Oset and L. L. Salcedo, Nucl. Phys. A **468**, 631 (1987).
[8] O. Buss, T. Gaitanos, K. Gallmeister, H. van Hees, M. Kaskulov, O. Lalakulich, A. B. Larionov, T. Leitner *et al.*, Phys. Rep. **512**, 1 (2012).
[9] S. J. Barish, M. Derrick, T. Dombeck, L. G. Hyman, K. Jaeger, B. Musgrave, P. Schreiner, R. Singer *et al.*, Phys. Rev. D **19**, 2521 (1979); G. M. Radecky, V. E. Barnes, D. D. Carmony, A. F. Garfinkel, M. Derrick, E. Fernandez, L. Hyman, G. Levman *et al.*, *ibid.* **26**, 3297 (1982).
[10] T. Kitagaki *et al.*, Phys. Rev. D **34**, 2554 (1986); T. Kitagaki, H. Yuta, S. Tanaka, A. Yamaguchi, K. Abe, K. Hasegawa, K. Tamai, H. Sagawa *et al.*, *ibid.* **42**, 1331 (1990).
[11] O. Lalakulich, T. Leitner, O. Buss, and U. Mosel, Phys. Rev. D **82**, 093001 (2010).
[12] K. M. Graczyk, J. Żmuda, and J. T. Sobczyk, Phys. Rev. D **90**, 093001 (2014).
[13] A. A. Aguilar-Arevalo *et al.* (MiniBooNE Collaboration), Phys. Rev. D **83**, 052007 (2011).
[14] B. Eberly *et al.*, arXiv:1406.6415 [hep-ex].
[15] T. Golan, C. Juszczak, and J. T. Sobczyk, Phys. Rev. C **86**, 015505 (2012).
[16] J. Nieves, I. R. Simo, and M. J. Vicente Vacas, Phys. Rev. C **83**, 045501 (2011).
[17] R. Gran, J. Nieves, F. Sanchez, and M. J. Vicente Vacas, Phys. Rev. D **88**, 113007 (2013).
[18] J. T. Sobczyk, Phys. Rev. C **86**, 015504 (2012).
[19] J. T. Sobczyk and J. Żmuda, Phys. Rev. C **87**, 065503 (2013).
[20] D. Rein and L. M. Sehgal, Nucl. Phys. B **223**, 29 (1983).
[21] C. Berger and L. M. Sehgal, Phys. Rev. D **79**, 053003 (2009).
[22] A. Higuera *et al.*, Phys. Rev. Lett. **113**, 261802 (2014).
[23] O. Lalakulich and U. Mosel, Phys. Rev. C **87**, 014602 (2013).
[24] P. A. Rodrigues, arXiv:1402.4709v1 [hep-ex].
[25] C. Andreopoulos *et al.*, Nucl. Instrum. Meth. A **614**, 87 (2010).
[26] K. M. Graczyk, D. Kielczewska, P. Przewlocki, and J. T. Sobczyk, Phys. Rev. D **80**, 093001 (2009).
[27] B. Eberly (private communication).
[28] M. J. Wilking, Ph.D. thesis, University of Colorado, Boulder (2009).
[29] C. Wilkinson, P. Rodrigues, S. Cartwright, L. Thompson, and K. McFarland, Phys. Rev. D **90**, 112017 (2014).